1962–1972 *Nucleic Acids Research, 2009, Vol. 37, No. 6* *Published online 10 February 2009*
doi:10.1093/nar/gkp071

Single-molecule analysis reveals two separate DNA-binding domains in the *Escherichia coli* UvrA dimer

Koen Wagner[1], Geri Moolenaar[1], John van Noort[2] and Nora Goosen[1,*]

[1]Laboratory of Molecular Genetics, Leiden Institute of Chemistry, Leiden University, Einsteinweg 55, 2333 CC, Leiden and [2]Physics of Life Processes, Leiden Institute of Physics, Leiden University, Niels Bohrweg 2, 2333 CA, Leiden, the Netherlands

Received December 17, 2008; Revised January 23, 2009; Accepted January 26, 2009

ABSTRACT

The UvrA protein is the initial damage-recognizing factor in bacterial nucleotide excision repair. Each monomer of the UvrA dimer contains two ATPase sites. Using single-molecule analysis we show that dimerization of UvrA in the presence of ATP is significantly higher than with ADP or nonhydrolyzable ATPγS, suggesting that the active UvrA dimer contains a mixture of ADP and ATP. We also show that the UvrA dimer has a high preference of binding the end of a linear DNA fragment, independent on the presence or type of cofactor. Apparently ATP binding or hydrolysis is not needed to discriminate between DNA ends and internal sites. A significant number of complexes could be detected where one UvrA dimer bridges two DNA ends implying the presence of two separate DNA-binding domains, most likely present in each monomer. On DNA containing a site-specific lesion the damage-specific binding is much higher than DNA-end binding, but only in the absence of cofactor or with ATP. With ATPγS no discrimination between a DNA end and a DNA damage could be observed. We present a model where damage recognition of UvrA depends on the ability of both UvrA monomers to interact with the DNA flanking the lesion.

INTRODUCTION

Nucleotide excision repair (NER) is a universal DNA-repair mechanism that it is capable of repairing various chemically and structurally unrelated lesions. In bacteria, the proteins UvrA, UvrB and UvrC initiate NER by recognizing DNA lesions and catalyzing incisions on both sides of the damage (1,2). The current model for the mechanism of bacterial NER consists of the following steps: first, two UvrA proteins and two UvrB proteins associate to form the $UvrA_2B_2$ complex, which searches the DNA for potential damages. Initially UvrA will probe the DNA for presence of a damaged site and after detection of such a site it hands off the DNA to UvrB which then will verify if a lesion is present. After detection of a DNA lesion by UvrB, UvrA dissociates leaving the so-called pre-incision complex which has one UvrB subunit tightly bound to the lesion and the second subunit more loosely associated. UvrC subsequently displaces the second UvrB subunit from the pre-incision complex and incises the DNA, first at the 3′ side and then at the 5′ side of the damage.

In recent years structural and biochemical analysis of (mutant) UvrB proteins has shed considerable light on the process of damage recognition by UvrB. The protein uses a β-hairpin motif that inserts between the two DNA strands (3,4). It has been postulated that nucleotides are flipped behind this hairpin until a lesion is detected (5–8). Much less is known, however, about the role of UvrA in damage detection. Very recently, the crystal structure of the ADP-bound form of the *Bacillus stearothermophilus* UvrA dimer has been solved (9). Each monomer contains two ATP-binding sites belonging to the superfamily of ABC ATPases. In classical ABC ATPases, the ATP is bound at the interface of the dimer bridging the ATP-binding domain of one subunit with the signature domain of the other subunit (10). In UvrA, however, the ATP-binding sites are formed in an intramolecular fashion by the Walker A and Walker B motifs in the N-terminal part of the protein and the signature motif in the C-terminal part and *vice versa*. Still ATP has been shown to stimulate dimerization and it has been suggested that ATP hydrolysis results in monomerization (11,12). UvrA (in absence of UvrB) binds DNA with a preference for single-stranded or damaged DNA (13,14). This DNA binding is influenced by the presence of ATP, ADP and nonhydrolyzable ATP analogs (14,15). It has been proposed that the ATPase activity of UvrA results in dissociation of the protein from undamaged sites (11,16,17).

*To whom correspondence should be addressed. Tel: +31715274773; Fax: +31715274340; Email: n.goosen@chem.leidenuniv.nl

In this paper we analyze the UvrA protein at the single-molecule level using atomic force microscopy (AFM). We show that, in contrast to what was concluded from bulk measurements, dimerization of UvrA is stimulated by ATP hydrolysis, suggesting that the active UvrA dimer contains a mixture of ADP and ATP. AFM analysis of UvrA bound to a DNA substrate containing a defined lesion revealed that ATP is not required for damage detection. We also present evidence that each monomer of the UvrA dimer has a separate DNA-binding domain and discuss a model where simultaneous binding of the two monomers provides damage discrimination.

MATERIALS AND METHODS

Proteins and chemicals

UvrA and UvrB were purified as described (18). Ku70/80 was generously donated by Dr. Roland Kanaar (Erasmus University, Rotterdam). ADP, ATP, ATPγS, Creatine Phosphate (CP) and Creatine Kinase (CK) were purchased from Roche.

Luciferase assay

Luciferase based detection of bound ATP or ADP was performed using the ATP Bioluminescent Assay Kit (Sigma). A sample of 0.1 μM UvrA (100 μl) was boiled for 10 min at 100°C to release any bound nucleotides. To measure ADP content, ADP was converted into ATP by CK (0.16 μg/μl) and CP (20 mM) by incubating 15 min at 37°C. After CP + CK treatment, samples were boiled again for 10 min at 100°C to denature CK before measuring their ATP content. Calibration samples containing the same buffer with 5, 10 or 20 pmol ATP or ADP were treated similarly.

Luminescence was measured using a Trilux 1450 MicroBeta Wallac Luminometer (Perkin-Elmer).

DNA substrates

A 678-bp DNA fragment with Thymine-N3-Menthol (Menthol) lesion incorporated at position 340 was prepared as described (19). The bottom strand was obtained by PCR on DNA isolated from the yeast gene URA-3, using the forward primer U4 (CGGTAATCTCCGAGCA GAAGGAAGAACGAAGG) and the 5′-biotin-labeled reverse primer U5 (TTTCCCGGGTCGCTCTTCGCAA TGTCAACAGTACCC) followed by purification of the single strand with streptavidin-coated magnetic beads. The 313-nt top strand was isolated in a similar way using primers U4 and 5′-biotin-labeled reverse primer Bio1078B (TTTGGGACCTAATGCTTCAAC). The 313-nt top strand and 50-nt oligo containing the Menthol lesion were annealed to the bottom strand and after ligation the incomplete top strand was extended with Sequenase version 2.0 DNA polymerase (USB). Finally, the DNA was removed from the beads by cleavage with SmaI, resulting in a blunt-end fragment of 678-bp with a Menthol damage in the center of the fragment.

The undamaged 678-bp DNA fragment was obtained in an identical way with exception that the 313-nt top strand was ligated with the corresponding undamaged 50-nt oligo prior to extension with polymerase.

The 1020-bp DNA fragment for Ku70/80 binding was obtained by PCR on the URA-3 gene with forward primer U3 (GAAGGAAGAACGAAGGAAGGAGC) and reverse primer UH4 (TTTCCGGGGGGCCCGGGTAA TAACTGATATAATT).

AFM Imaging

For visualization of UvrA monomers and dimers, the UvrA protein (20 nM) was incubated for 5 min at 37°C in 20 μl UV-Endo buffer (100 mM KCl, 10 mM $MgCl_2$, 50 mM Tris, pH 7.5). Ku70/80 heterodimer was incubated for 5 min at 37°C in 20 μl Ku-B (50 mM KCl, 10 mM $MgCl_2$, 50 mM HEPES, pH 7.8). When indicated, nucleotide cofactors were added in a concentration of 1 mM. After incubation 5 μl from the sample was directly deposited onto freshly cleaved mica (Spruce Pine mica Co.). After 30 s, the mica was rinsed with Milli-Q water and gently dried with a stream of air.

For visualization of UvrA–DNA complexes, UvrA (20 nM) was incubated in 10 μl UV-endo buffer with 50 ng of the damaged or undamaged 678-bp DNA for 10 min at 37°C and Ku70/80 heterodimer was incubated in 10 μl Ku-B with 50 ng of the 1020-bp DNA for 10 min.

Deposition of UvrA–DNA complexes and simultaneous deposition of UvrA–DNA and Ku70/80–DNA complexes was performed as described by Verhoeven *et al.* (19) using a 10 mM $MgCl_2$, 10 mM HEPES, pH 7.8 deposition buffer.

Imaging was performed with a Nanoscope III instrument (Digital Instruments), equipped with an E-scanner, using tapping mode in air. OMCL-AC240TS MicroCantilever tapping mode cantilevers (Olympus) with a spring constant of 2 N/m and a resonance frequency of 70 kHz were used for all imaging. All images of deposited proteins or protein–DNA complexes were collected at a scan rate of 2 Hz and a scan size of 1 μm^2 and 2 μm^2, respectively. The 3D-surface plot was generated using WSxM 2.2 software (20).

Calculation of protein complex volumes

Protein complex volumes were calculated with custom software written in LabView (National Instruments). Before calculating the volumes of deposited proteins and protein–DNA complexes, images were flattened by line subtraction of a polynomial fit to the height profile. Complex volumes were calculated by summing of the height at each pixel inside a circle around the mass center of a protein complex. Protein complexes were selected manually, after which the centers of mass were determined. The radius of the circle used for volume calculations was 9 pixels on images with 1 μm^2 size and 4 pixels on images with 2-μm^2 size.

Calculation of dimerization percentages and dissociation constants

Volume distribution histograms were made using OriginPro 7.5 software (OriginLab Co.). Two Gaussian curves were fitted to the distribution histograms, using

OriginPro 7.5 software. The percentage of dimers was calculated using the area under the curves of the monomer (M) and dimer (D) species [Equation (1)].

$$\%\text{dimers} = \left[\frac{\text{D}}{(\text{M}+\text{D})}\right] \times 100\% \quad \textbf{1}$$

The dissociation constant (K_d) of the UvrA dimer was calculated from the fraction of monomers as dimers [$f = 2D/(M + 2D)$], measured at different protein concentrations (c). K_d is equal to the inverse slope of the line fitted to a plot of $f/2\ (1 - f)^2$ versus c (adapted from ref. 21).

Generation of position distribution histograms

The position of UvrA complexes on a DNA contour was determined semi-automatically, using custom software written in LabView (National Instruments). DNA molecules were manually picked. The trajectory of the DNA was traced automatically by following its height contour. Only DNA contours with lengths within the standard deviations of the average DNA length were used for generating position distribution histograms. In our histograms, the 678-bp DNA substrate was divided into 20 bins. Only UvrA complexes with volumes within the standard deviations of the average UvrA-complex volume were used for generating position distributions histograms. UvrA complexes, that appeared to have bound to two DNA molecules, were excluded from the position distribution histograms.

The relative distance to the DNA center (RDC) was calculated as the absolute value of the quotient from the position (A) of a UvrA complex with the DNA contour length (L) minus 0.5 [Equation (2)]

$$\text{RDC} = \text{Abs}\left(\left[\frac{A}{L}\right] - 0.5\right) \quad \textbf{2}$$

The probability distribution (P_i) of UvrA complexes at each position was calculated by dividing the number of complexes at a given relative position bin (n_i) with the total number of UvrA complexes bound (Σn_i) multiplied by the number of basepairs per bin ($N_{bp,bin}$) [Equation (3), adapted from ref. 22].

$$P_i = \frac{n_i}{(N_{\text{bp,bin}} \times \sum n_i)} \quad \textbf{3}$$

UvrA complexes with their center of mass <10% (RDC > 0.4) away from the end of the DNA contour were designated to have bound to a DNA end. By visual inspection, it was confirmed that UvrA complexes, located at <10% away from a DNA end, were located at a DNA end.

Calculation of site-specific binding

The percentage of complexes bound to the DNA damage was calculated by dividing the number of complexes bound to the DNA damage by the total number of complexes detected. The number of complexes on the DNA damage was calculated by counting the number of complexes bound <10% (RDC < 0.1) away from the middle of the DNA contour, corrected for the amount of complexes bound to nonspecific sites <10% away from the center. This correction was done by subtracting the average amount of complexes bound to an equal amount of nonspecific sites (0.2 < RDC < 0.3) from the number of complexes bound to the damage.

The percentage of complexes bound to a DNA end was calculated by a similar method.

Determination of binding specificity

The binding specificity (S) for the DNA damage and DNA end was calculated by multiplying the ratio of the percentages of complexes on a specific site (P_{sp}) and on nonspecific sites (P_{nsp}) with the amount of nonspecific binding sites (N) [Equation (4), as described in ref. 22]. On the undamaged DNA: $N = 676$ bp, excluding both ends; on the damaged DNA, $N = 675$ bp, excluding both ends and the DNA damage.

$$S = N\left(\frac{P_{\text{sp}}}{P_{\text{nsp}}}\right) + 1 \quad \textbf{4}$$

RESULTS

UvrA forms dimers in the absence of a nucleotide cofactor

Previous studies have shown a linear relationship between the volume of a protein as determined by AFM and its molecular weight (21). We therefore have used AFM to analyze the dimerization of the UvrA protein. AFM images, taken from depositions of 20 nM UvrA in the absence of a nucleotide cofactor, revealed complexes with two different sizes. An example of such an AFM image is shown in Figure 1. A histogram of all the obtained complex volumes shows two separate populations with distinctly different volumes (Figure 2A). The average complex volume of each population was determined using a calibration curve with UvrB monomers (76 kDa), UvrB dimers (152 kDa) and Ku70/80 (155 kDa) as reference proteins. The thus obtained molecular weights of the UvrA populations were 111.2 kDa and 223.2 kDa (Figure 2B), which correlate very well with the theoretical molecular weight of the UvrA monomer (110 kDa) and UvrA dimer (220 kDa), respectively. The percentage of dimers in the absence of a cofactor was determined at three different UvrA concentrations (Table 1) and from a global fit of these data (described in 'Materials and Methods' section) a dissociation constant (K_d) for the UvrA dimer of 36 nM could be calculated (Supplementary Figure 1).

To test whether the observed dimerization might be due to ADP and/or ATP that was co-purified with the UvrA protein, we measured the amount of cofactor present in the UvrA preparation using the Luciferase assay described in 'Materials and methods' section. With this method the ATP concentrations can be measured directly and for measuring the ADP concentration, ADP was first converted to ATP using CK. As shown in Figure 3 no

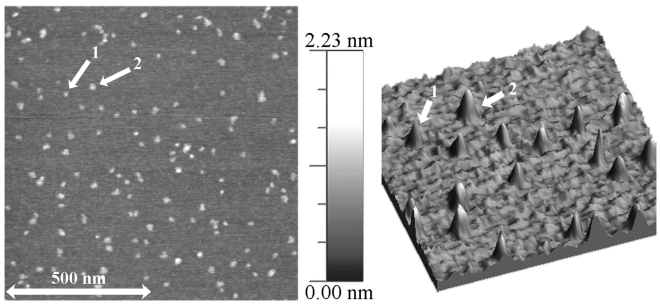

Figure 1. Representative AFM image (left) of 20 nM UvrA without cofactor and surface plot (right) of an area within the AFM image. Image size is 1×1 μm, with the gray scale ranging from 0.0 to 2.23 nm (from dark to bright); surface plot area is 400×400 nm, with the same gray scale. Arrow 1 points to a small (monomer) UvrA complex, arrow 2 points to a large (dimer) UvrA complex.

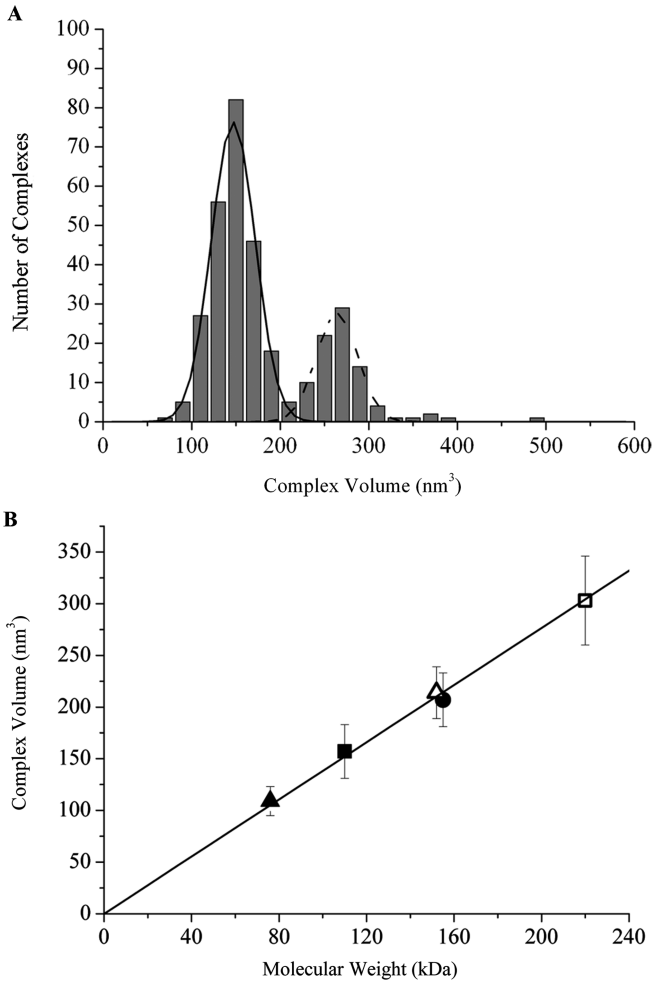

Figure 2. (**A**) Volume distribution histogram for UvrA (20 nM, without cofactor). The solid line is a Gaussian curve fitted to the volume data of the small (monomer) complex, the dashed line is a Gaussian curve fitted to the volume data of the large (dimer) complex. The area under each Gaussian curve represents each complex's population. **(B)** Calibration curve of calculated protein volume versus molecular weight. Shown are: UvrB monomer (closed triangle: 109 nm^3, 76 kDa), UvrA small (monomer) complex (closed square: 157 nm^3, 111 kDa), Ku70/80 (closed circle: 207 nm^3, 155 kDa), UvrB dimer (open triangle: 214 nm^3, 152 kDa) and UvrA large (dimer) complex (open square 303 nm^3, 223 kDa). The line represents a linear fit to the data, which is described by the following equation: $V = 1.38 \times MW$. The error bars represent the standard deviation in the average volumes calculated from different experiments.

detectable amounts of ATP or ADP are present in the purified UvrA protein, confirming that indeed UvrA can form dimers in the absence of cofactor.

ATP hydrolysis stimulates dimerization of UvrA

Next, we determined the percentage of UvrA dimers in the presence of different cofactors. Addition of ATP led to a significant increase in dimerization, reducing the K_d over 10-fold (Table 1). Apparently, an ATP-induced conformational change in the protein stabilizes the dimer. Addition of the nonhydrolyzable ATP analog ATPγS, however, did not alter the dimerization of UvrA (Table 1). Also in the presence of another nonhydrolyzable analog, AMP-PNP, the dimerization levels of UvrA remained unaltered (data not shown). UvrA has been shown to bind these nonhydrolyzable cofactors since they are potent competitive inhibitors of the ATPase activity of UvrA (ref. 11 and our lab, data not shown). This strongly suggests that it is not the binding of ATP that stimulates formation of UvrA dimers, but the hydrolysis of ATP to ADP. To test this model further, dimerization levels of UvrA were studied using conditions where UvrA is able to bind, but not hydrolyze ATP. For this purpose UvrA was incubated at 4°C after which the protein mixture was deposited on freshly cleaved mica, which was precooled at 4°C. At 4°C, no ATPase activity of UvrA was detected in an ATPase assay (data not shown), but at this temperature UvrA has been shown to bind ATP (23). Indeed under this nonhydrolyzing condition, addition of ATP does no longer stimulate UvrA dimerization (Table 1), confirming that dimerization of UvrA is stimulated by hydrolysis of ATP.

Addition of ADP also led to an increase in dimerization of UvrA, but not to the levels observed in the presence of ATP. One explanation for this difference might be that upon hydrolysis of ATP the generated free phosphate (PO_4^{3-}) remains bound to the protein and that the repulsion between ADP and this phosphate induces the specific conformation that stabilizes the dimer interface. We therefore also measured the percentage of dimers in the presence of ADP and 100-mM phosphate, but no difference in dimerization levels could be observed (Table 1). A more likely explanation for the observed difference between ADP and ATP therefore is that not all four ATP molecules are hydrolyzed in the UvrA dimer and that the most stable dimer is generated when the four ATP-binding sites are partly occupied with ADP and partly with ATP. To confirm this, we analyzed the dimerization level upon addition of a mixture of ADP and ATPγS. In the presence of this mixture, a higher amount of UvrA dimers was found than with either ADP or ATPγS alone (Table 1), showing that indeed the UvrA dimer is most stable when the ATPase sites

Table 1. UvrA dimerization in presence of different nucleotide cofactors

Cofactor	% Dimers			K_d (nM)
	5 nM	20 nM	50 nM	
None	26.1 ± 2.3	29.1 ± 3.5	36.3 ± 3.0	36
ATP	52.2 ± 4.3	67.2 ± 1.7	76.9 ± 2.2	1.9
ATPγS	26.7 ± 0.3	30.0 ± 4.4	34.3 ± 2.3	39
ADP	46.4 ± 0.5	48.7 ± 2.5	54.0 ± 2.2	11
None, 4°C	ND	30.0 ± 1.9	ND	ND
ATP, 4°C	ND	30.1 ± 1.8	ND	ND
ADP + P_i	ND	48.8 ± 1.0	ND	ND
ADP + ATPγS	ND	55.0 ± 1.0	ND	ND
UvrB, no cofactor	10.0 ± 0.5	11.0 ± 0.1	26.7 ± 1.2	83

Dimer percentages were calculated using volume distribution histograms as described in 'Materials and methods' section.
Data were obtained from at least two independent experiments.
Plots used for K_d determination are shown in Supplementary Figure 1.
ND = Not determined

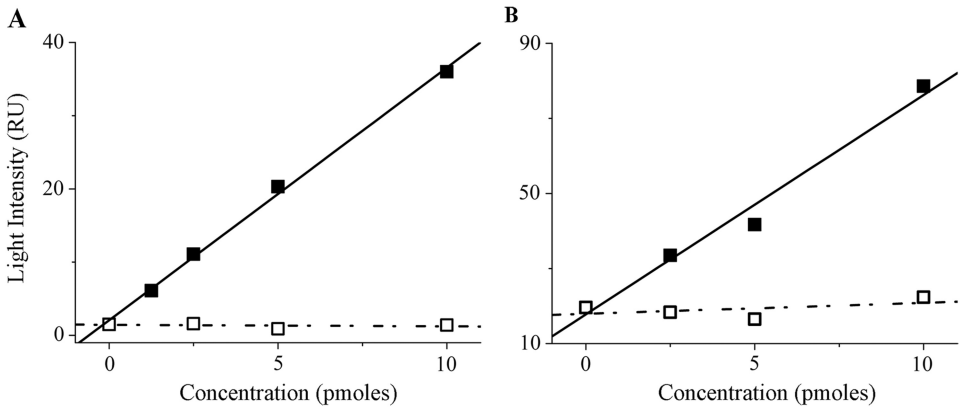

Figure 3. Determination of ATP and ADP content of UvrA. (**A**) Luciferase assay of samples containing ATP (closed squares) or UvrA (open squares). (**B**) Luciferase assay of samples containing ADP (closed squares) or UvrA (open squares) after treatment with Creatine Kinase and Creatine Phosphate. Light intensities are expressed in Relative Units (RU).

are partly occupied with ADP and partly with ATP. The dimerization level of UvrA in the presence of ADP and ATPγS, however, was lower than with ATP. This can be explained by random occupation of the ATPase sites by ADP and/or ATPγS, resulting in a mixture of UvrA dimers with varying stabilities, whereas ATP hydrolysis in the UvrA dimer will lead to a defined cofactor occupation.

Since we used UvrB monomers and dimers in our equilibration curve we could also determine the dimerization of this protein. In the absence of cofactor, a K_d of 83 nM was found for *Escherichia coli* UvrB (Table 1 and Supplementary Figure 2). This is significantly higher as reported for the *Bacillus caldotenax* UvrB protein (K_d of 5 nM), which was determined using the same method (24). Most likely this difference in stability is due to the thermophilic origin of the *B. caldotenax* protein.

UvrA binds undamaged DNA preferentially at the end

To determine whether both monomers and dimers of UvrA can bind DNA we used AFM to measure the size of the UvrA–DNA complex formed on undamaged DNA. The volumes of UvrA–DNA complexes (located on a 678-bp DNA fragment) were determined and compared with the volumes of simultaneously deposited Ku70/80–DNA complexes (located on a 1020-bp DNA fragment). The volumes of the UvrA complexes on DNA appeared to be larger than that of the free UvrA monomer and dimer (Figures 2A and 4), due to the contribution of the DNA. Therefore, the volume of the Ku70/80–DNA complex was used as a reference. Simultaneous deposition of UvrA bound to a 678-bp fragment with the 1020-bp fragment without added Ku70/80 revealed that ~10% of the UvrA complexes were detected on the longer fragment. Less than 10% of the Ku70/80 complexes were detected on the other DNA fragment after simultaneous deposition of the Ku70/80-bound 1020-bp fragment and the free 678-bp DNA, as was also demonstrated by Verhoeven *et al.* (25). Histograms obtained from the volume distributions of both complexes (Figure 4) reveal that the UvrA–DNA complex has a size corresponding to the molecular weight of 200–224 kDa (Table 2). Under all cofactor conditions we never detected a complex corresponding

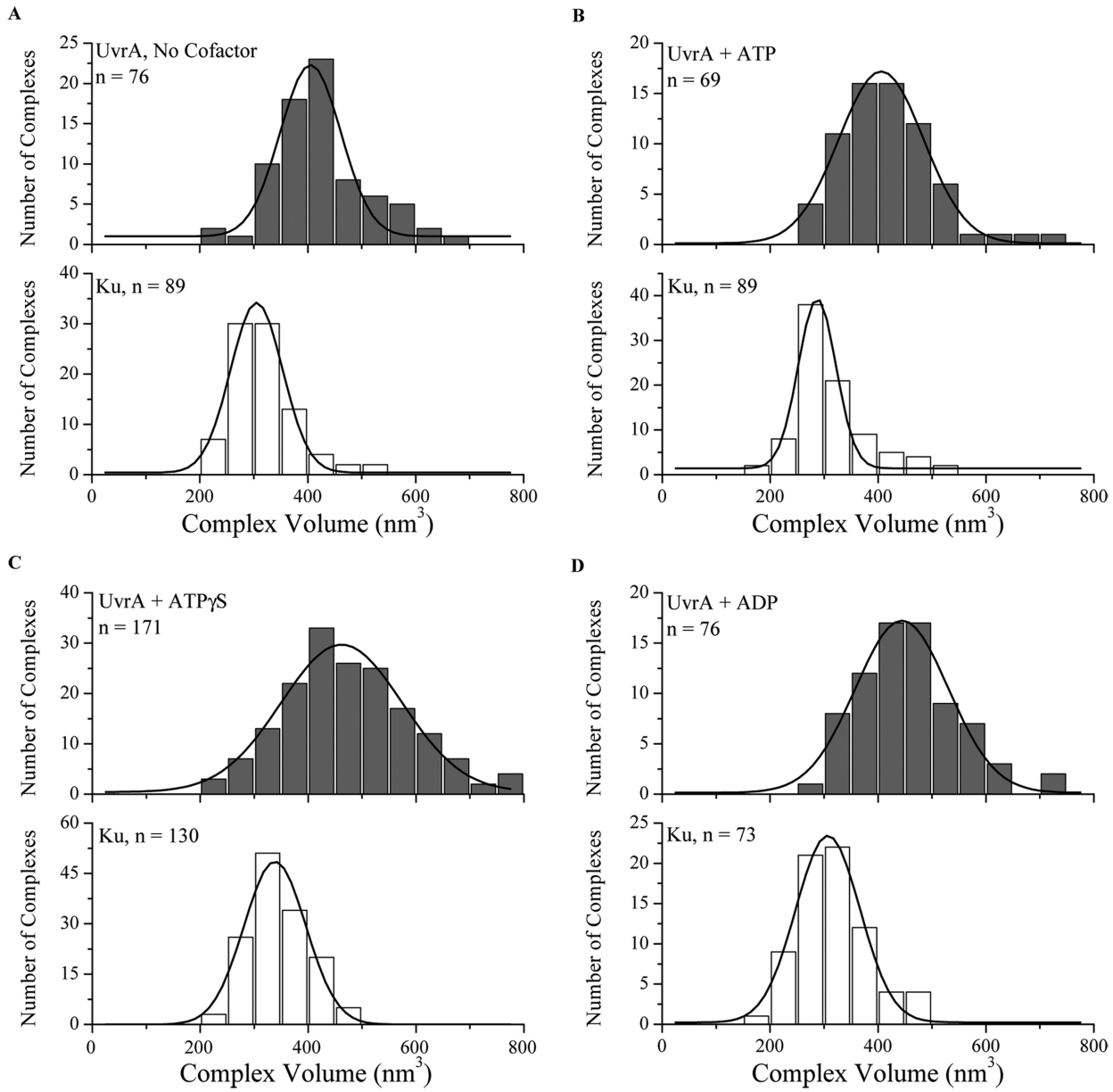

Figure 4. Volume distribution histograms for UvrA–DNA complexes (gray bars) incubated in absence of cofactor (**A**) and in presence of ATP (**B**), ATPγS (**C**) or ADP (**D**) and simultaneously deposited Ku70/80–DNA complexes (white bars). The total number of UvrA and Ku complexes measured is shown in each plot. The black lines are Gaussian fits to the volume data.

to the size of a UvrA monomer, which would be smaller than the Ku70/80–DNA complex. This unambiguously shows that UvrA only binds DNA as a dimer, even in the absence of cofactor where 70% of the protein was shown to be in the monomeric form.

Analysis of the position of UvrA on the DNA revealed that the majority of the UvrA–DNA complexes were located at the end of the DNA fragment (Figure 5A). The distribution of internal-bound UvrA versus end-bound protein was independent of the cofactor used (Figure 6 and Table 3), showing that the cofactor does not play a role in the discrimination between internal sites and DNA ends. Most likely the partly single-stranded

Table 2. Molecular weight of UvrA on DNA

Cofactor	Average volume UvrA complex on DNA (nm^3)	Average volume Ku complex on DNA (nm^3)	Calculated molecular weight for UvrA on DNA (kDa)
None	408 ± 9	316 ± 6	200 ± 4
ATP	406 ± 3	287 ± 3	219 ± 2
ATPγS	462 ± 6	338 ± 3	212 ± 3
ADP	444 ± 4	307 ± 2	224 ± 2

The molecular weight of UvrA–DNA was calculated using the volume of Ku (155 kDa) as a reference.
MW = 155 × Vol UvrA-DNA/Vol Ku-DNA.
Average volumes were calculated from the Gaussian fits shown in Figure 4.

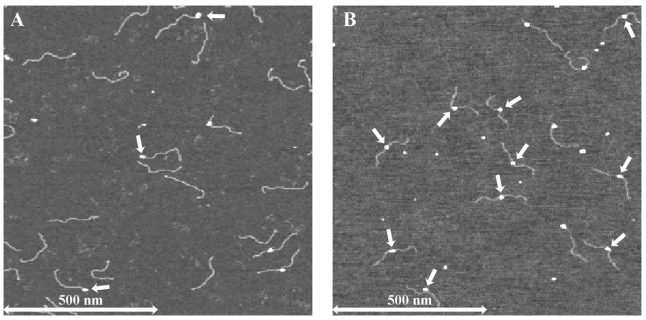

Figure 5. (**A**) Representative AFM image of UvrA complexes on 678-bp undamaged DNA in the absence of cofactor. Image size is $1 \times 1\,\mu m$, with the gray scale ranging from 0.0 to 4.0 nm (from dark to bright). The white arrows indicate UvrA–DNA complexes, where UvrA is bound to a DNA end. (**B**) Representative AFM image of UvrA–DNA complexes on 678-bp DNA containing a Menthol lesion at basepair 340 in the absence of cofactor. Image size is $1 \times 1\,\mu m$, with the gray scale ranging from 0.0 to 4.0 nm (from dark to bright). The white arrows indicate UvrA–DNA complexes, where UvrA is bound to the Menthol lesion.

nature of DNA ends enhances the affinity for UvrA. The specificity of UvrA for a DNA end versus an internal site was calculated to be a factor ~400 [Equation (4), 'Materials and methods' section].

When analyzing the DNA complexes the most striking observation was that about 4% of the end-bound UvrA proteins formed a bridge with a second DNA end (Figure 7A), either on the same DNA (panels 1 and 5) or with another DNA molecule (panels 2–4). This was observed in absence and presence of the different cofactors and in all cases the volume of the bridging protein corresponded to one UvrA dimer. Apparently, the same UvrA dimer is capable of binding to two different targets, most likely using the DNA-binding domain of one subunit to interact with one DNA end. This could mean that also in the other UvrA dimers bound to DNA ends without forming a bridge only one of the monomers contacts the DNA. With a much lower frequency (around 1%) also complexes could be found with a UvrA dimer bound to both a DNA end and an internal DNA binding

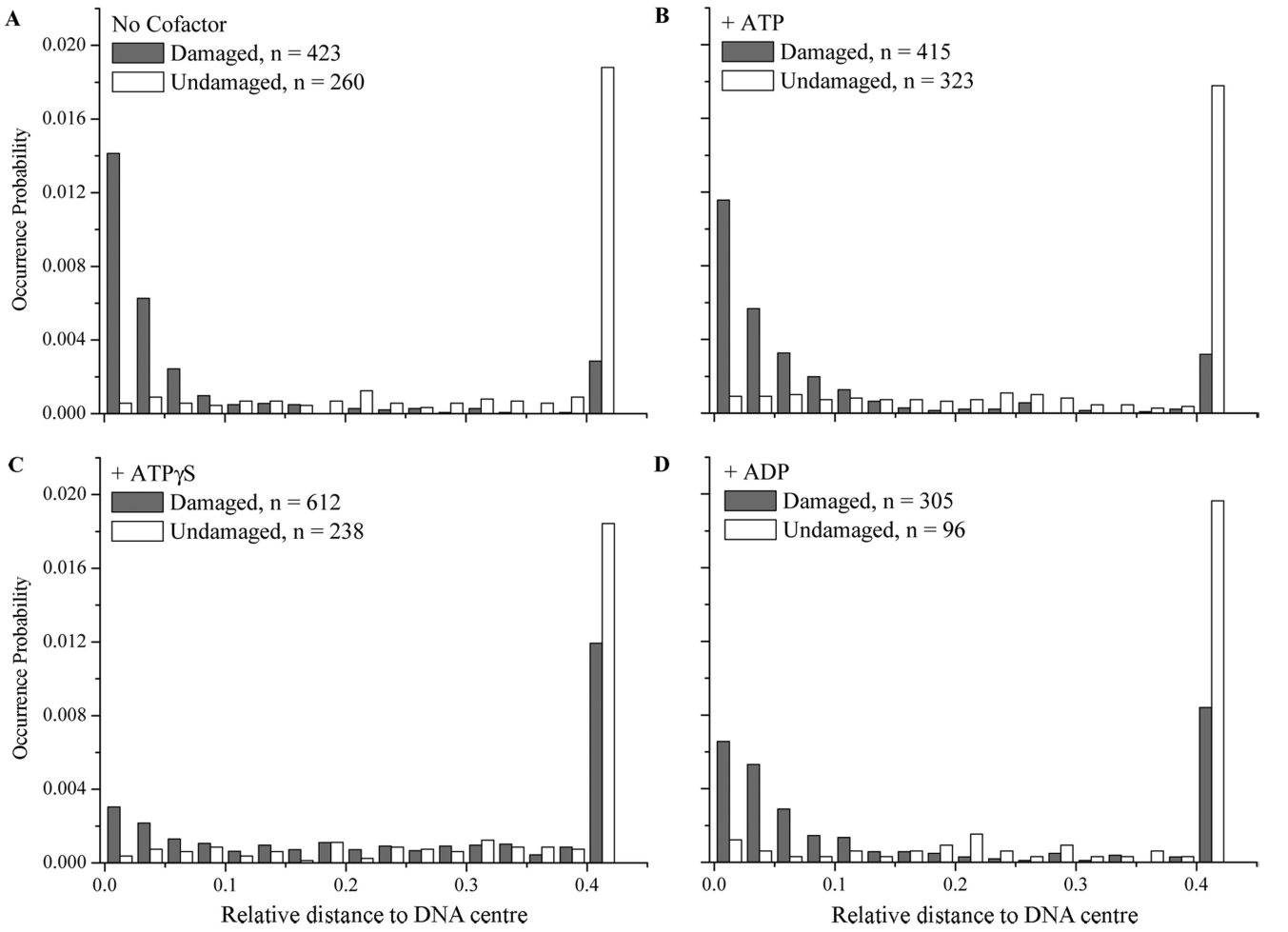

Figure 6. Distribution of UvrA complexes on damaged (gray bars) and undamaged DNA (white bars), when incubated in absence of cofactor (**A**) and in presence of ATP (**B**), ATPγS (**C**) or ADP (**D**). The total number of complexes counted is shown in each plot. The occurrence probability is the observed probability of UvrA binding within a range of positions, and the complex position is shown as relative distance to the DNA center (see 'Materials and methods' section). Complexes with relative distance to the DNA center >0.4 are defined as bound to a DNA end.

site (Figure 7A, panel 6). The lower affinity for internal sites compared to DNA ends can explain the lower occurrence, but their presence suggests that also when bound to internal sites the UvrA dimer uses only one subunit to contact the DNA.

Preference for damaged site is dependent on the type of cofactor

To test the specific binding of UvrA to a DNA damage we constructed the same 678-bp DNA fragment as used for the binding of undamaged DNA, but now having a Menthol adduct attached to the N3 position of a thymine in the center of the DNA fragment (see 'Materials and Methods' section). An example of an AFM image of UvrA bound to this substrate is shown in Figure 5B. As for the UvrA bound to undamaged DNA all complexes formed on the damaged DNA substrate corresponded to the size of the UvrA dimer irrespective of the type of cofactor or location of the protein on the DNA. In the absence of cofactor or with ATP a very high preference of UvrA for the damaged site is observed (Figure 5A and B) with 75–78% of the DNA molecules having the protein bound at the center of the fragment and only 7–8% at the DNA end (Table 4). From these distributions a preference for binding the Menthol damage versus a nondamaged site was calculated to be ~3500. With ADP there is also a preference to bind the damaged site, but this frequency is significantly lower (53.1 ± 5.8%) and a substantial amount (24.9 ± 1.1%) is still found at the DNA ends (Table 4). With ATPγS binding to the damage is even further reduced (13.4 ± 3.1%) and is lower than the percentage of complexes at the end (31.2 ± 6.3%). However, as each DNA fragment contains two ends this means that the binding affinities for a DNA damage or a DNA end are similar in the presence of ATPγS.

In all the depositions, regardless of the type of cofactor we again observed complexes in which two DNA ends are bridged by one UvrA dimer (Figure 7B, panels 1–4) or where UvrA bridges an end and an internal site (panels 5 and 6). Occasionally, these internal sites were located in the center of the fragment (panel 6), but the occurrence of these complexes was too low to determine whether in these complexes UvrA is indeed bound to the damaged site. In none of the depositions, however, we could find complexes with UvrA simultaneously bound to two damaged sites, not even under conditions where

Table 3. Site-specific binding of UvrA on undamaged DNA

Cofactor	On end (%)	On Nonspecific site (%)
None	56.2 ± 5.9	43.8 ± 5.9
ATP	50.5 ± 4.5	49.5 ± 4.5
ATPγS	54.2 ± 6.9	46.8 ± 6.9
ADP	55.2 ± 5.9	44.8 ± 5.9

Table 4. Site-specific binding of UvrA on damaged DNA

Cofactor	On damage (%)	On end (%)	On nonspecific site (%)
None	78.5 ± 2.7	6.9 ± 1.4	14.6 ± 1.3
ATP	75.9 ± 1.9	8.0 ± 0.3	16.1 ± 2.2
ATPγS	13.4 ± 3.1	31.2 ± 6.3	53.4 ± 10.9
ADP	53.1 ± 5.8	24.9 ± 1.1	22.0 ± 5.9

Percentages were calculated using complex distribution histograms as described in 'Materials and Methods' section.
Data were obtained from at least two independent experiments.

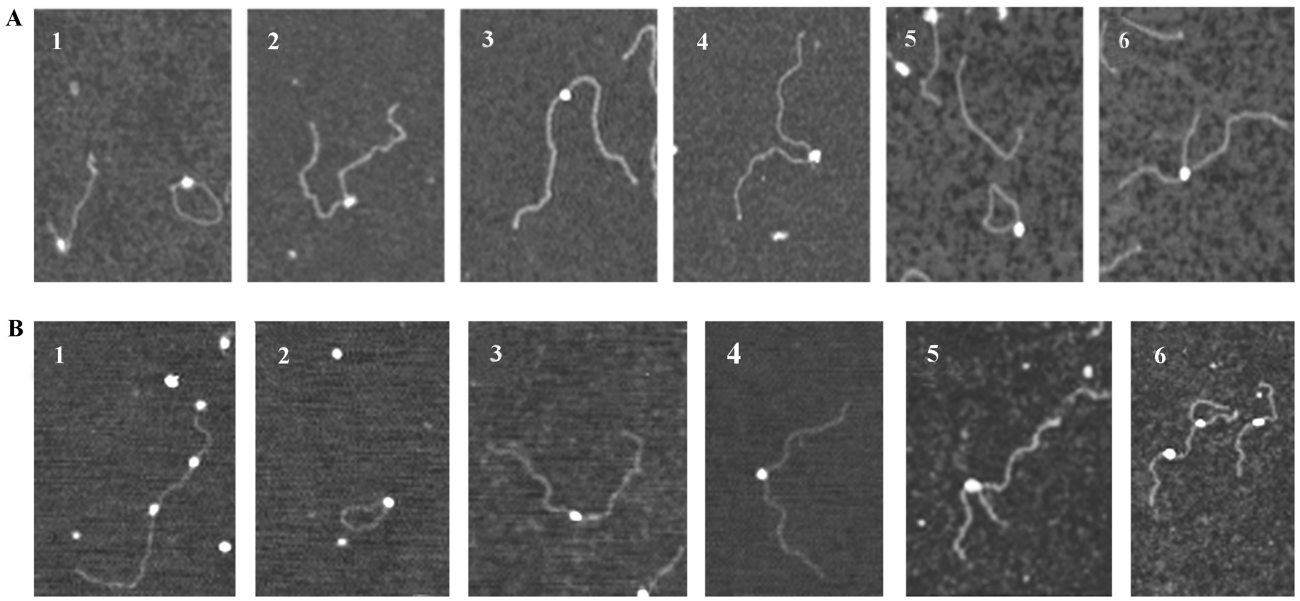

Figure 7. Examples of UvrA complexes simultaneously binding to two separate DNA-binding sites on undamaged DNA (**A**) and on damaged DNA (**B**).

damage-specific binding is much higher than end-binding (i.e. in the absence of cofactor or with ATP). Apparently, when bound to a damaged site the UvrA dimer is much less capable of making DNA bridges, suggesting that when bound to a damage both monomers are engaged in making contact with the DNA around the damaged site. When, on the other hand, the UvrA dimer has bound a DNA end, only one monomer interacts with the DNA, leaving the second subunit in a mobile state allowing it to bind another DNA target.

Our model also explains why DNA-end binding involving only one monomer is not dependent on the cofactor whereas damage-specific binding is. Most likely the type of cofactor influences the orientation of the two monomers in the dimer. Only in the absence of cofactor or in the presence of ATP (i.e. in the ATP/ADP mixed form) the orientation of the two monomers is optimal for simultaneous interaction with DNA at a damaged site.

DISCUSSION

In classical dimeric ABC ATPases, the dimerization of the protein is stimulated by binding of ATP at the dimer interface (10). In the UvrA dimer, however, the nucleotides are not located at the dimer interface and it has been proposed that ATP binding and hydrolysis regulate dimerization indirectly via rearrangement of the ATPase domains (9). In this paper we show, using single-molecule analysis that that the most stable dimer of UvrA contains a mixture of ADP and ATP, which is formed upon ATP hydrolysis. This is in contrast to previously presented data that suggested that ATP hydrolysis by UvrA would lead to monomerization of the protein (11). In these experiments, however, the oligomerization of UvrA was investigated using sedimentation and gel filtration analysis, which did not allow quantitative analysis of individual UvrA molecules. Moreover, the separation of monomers and dimers in these batch experiments is likely to influence the monomer-dimer equilibrium, whereas the rapid and irreversible deposition of protein onto mica for AFM analysis traps the oligomeric state of the protein in solution. The percentage of dimers that we find upon ATP hydrolysis is significantly higher than with UvrA fully occupied with ADP, indicating that the dimer is stabilized by the presence of a mixture of ADP and ATP in the protein. Most likely it is this ATP/ADP mixed form that will subsequently search the DNA for presence of damage. This mixed form could either be a symmetrical dimer with each monomer containing one ADP and one ATP or an asymmetrical dimer with one subunit containing two ADP and the other two ATP molecules.

AFM analysis of UvrA complexes on undamaged DNA revealed that UvrA binds DNA as a dimer with a strong preference for DNA ends. Most likely UvrA recognizes a DNA end as a potential damage because of partial strand separation at the end of a fragment, since the protein has been shown to have a high affinity for single-stranded DNA (13,14). The ability to preferentially bind to DNA ends was also demonstrated for *B. caldotenax* UvrA (26), but the authors restricted their analysis to UvrA in the presence of ATP. Remarkably, we found that the percentage of complexes that bound to the ends of the undamaged DNA substrate was independent of the cofactor used. Since 'finding' these DNA ends is expected to require multiple rounds of association and dissociation from nonspecific sites, this means that ATP binding or hydrolysis is not required for dissociation from nondamaged DNA. It has been suggested that dissociation of UvrA from undamaged sites is accompanied by monomerization of the protein dimer (16). The rapid fixation of protein–DNA complexes for AFM analysis would allow detection of UvrA-monomers associated with DNA. However, all complexes on the DNA visualized by AFM, irrespective of their location and irrespective of the cofactor, have the size of a UvrA dimer. This suggests that UvrA dissociates from DNA as a dimer and not via a monomeric intermediate state.

In contrast to the recognition of a DNA end, the recognition of the internal located Menthol-lesion by UvrA did show cofactor dependency. Without cofactor or with ATP more than 75% of the complexes were located at the site of the damage. With ADP damage-specific binding was somewhat reduced, but still significantly higher than end binding. With ATPγS, however, the protein was no longer capable of discriminating between a DNA end and a damaged site, although both were still preferred over a nondamaged site. The binding specificity for the Menthol-lesion, calculated for UvrA with ATP or without cofactor is ~3500, which is in the same order of magnitude as the binding specificity of UvrA that was calculated using bulk methods. Both with DNAse footprinting on a psoralen adduct (13) and with nitrocellulose filter binding on UV damaged DNA (16), the preference for the damage versus a nondamaged site was determined to be around a factor of 1000. The observed preferential binding of UvrA to a Menthol damage in the presence of ADP and ATPγS (albeit with different specificity) is consistent with data obtained with a psoralen adducts (13,15). The binding specificities for UvrA in the presence of these cofactors was however not determined in these studies.

The difference in cofactor requirement for specific binding to DNA damages and to DNA ends suggests a difference in the mode in which UvrA binds to these sites. The AFM images with undamaged DNA revealed that frequently complexes could be detected where one UvrA dimer has simultaneously bound to two DNA ends, irrespective of cofactor. Very likely, in these complexes each DNA end is contacted by one of the monomers, suggesting that also in the complexes where UvrA is bound to one DNA end, only one of the monomers is recognizing this DNA end. Bridging UvrA dimers could also be detected between a DNA end and an internal site, indicating that transient interaction with a nondamaged site can also occur with one monomer. In none of the images, however, simultaneous binding of UvrA to two damaged sites was observed, not even under conditions where the majority of UvrA complexes were located on the site of the lesion. We therefore propose that on an internally located lesion UvrA binds the DNA with both subunits, each monomer making contact with DNA on either side of the lesion where base pairing is reduced.

The function of the cofactor in this damage specific binding would then be to position the two DNA-binding domains within the UvrA dimer. In the cofactor-free form of UvrA the contacts at the dimer interface are clearly reduced compared to the ATP/ADP mixed form, resulting in lower dimer stability. In both protein forms, however, the orientation of the two DNA-binding domains is such that they can simultaneously contact the DNA flanking a lesion. As a result the affinity for the Menthol lesion (where both subunits contact the DNA) is higher than the affinity for a DNA end (where one subunit contacts the DNA). In the ATPγS-bound dimer the DNA-binding domains of each subunit are not properly positioned to allow simultaneous binding within a short stretch of constrained DNA (i.e. two closely located DNA regions flanking the lesion). As a result, the ATPγS-containing UvrA dimer contacts the DNA at a lesion site with one subunit only, similar as on a DNA end. The conformation of the ATPγS-bound UvrA dimer does allow simultaneous contact of the monomers with two DNA ends, as these end-to-end bridges were also observed when this nonhydrolyzable ATP analog was present. This shows that in the ATPγS form the two DNA-binding regions are exposed, but since the two DNA-binding targets are not directly connected, a proper positioning of these binding regions is not needed to contact both targets simultaneously. Our model predicts that with ATPγS simultaneous binding to two damaged sites should be possible as well. The occurrence of damage-specific complexes with ATPγS, however, is too low for detection of such bridged molecules.

The fully ADP-bound form of UvrA shows an intermediate activity: both the dimer stability and damage-specific binding are reduced compared to the ATP/ADP mixed form, but still higher compared to the ATPγS-bound form. Most likely, the positioning of the monomers in the ADP-bound dimer is intermediate between those of the ATPγS- and the ATP/ADP mixed form.

The structure of the ADP-bound dimer of *B. stearothermophilus* UvrA has recently been determined (9). In this dimer structure, two highly conserved regions could be indicated, one in each monomer, that are rich in positively charged amino acids. Base substitutions of these amino acids resulted in mutant proteins that were disturbed in DNA binding, indicating that the positively charged regions form an important DNA-binding surface (9). The mutant proteins were not only disturbed in damage-specific binding, but also in the binding to undamaged DNA (9), which as we show in this paper mainly represents binding to DNA ends. Apparently, UvrA uses the same motif for binding to a damage or a DNA end. In the structure of the ADP-bound UvrA dimer the two DNA-binding regions are separated by about 70 Å. This means that they are sufficiently spaced to allow binding to two DNA targets located on different DNA molecules. Until now, no structures of UvrA complexed with other cofactors are available, but it is conceivable that depending on the cofactor the two DNA-binding regions will take up different positions in the dimer thereby influencing the capacity to simultaneously interact with the DNA flanking a damage.

In summary, our data show that both the ATP/ADP mixed dimer and the cofactor free dimer can equally discriminate a lesion from an undamaged site, suggesting that the mixed cofactor composition of UvrA is not primarily associated with recognition of DNA damages. Most likely, the mixed cofactor composition is important for the subsequent step in DNA repair: loading of the UvrB protein. Analysis of UvrAB complexes containing UvrB-GFP and UvrB-YFP have shown that FRET between the UvrB proteins can only occur in the presence of ATP and not when this cofactor is absent (27). This indicates that the cofactors in UvrA (most likely in the ATP/ADP mixed form) not only orient the two DNA-binding motifs in the UvrA dimer but also the UvrB-binding domains thereby properly positioning the two UvrB subunits with respect to each other.

SUPPLEMENTARY DATA

Supplementary Data are available at NAR Online.

FUNDING

The Netherlands Organization for Scientific Research (NWO; grant number 700.52.706). Funding for open access charge: The Netherlands Organization for Scientific Research (NWO, grant number 700.52.706).

Conflict of interest statement. None declared.

REFERENCES

1. Van Houten,B., Croteau,D.L., DellaVecchia,M., Wang,H. and Kisker,C. (2005) 'Close fitting sleeves': DNA damage recognition by the UvrABC nuclease system. *Mutat. Res.*, **577**, 92–117.
2. Truglio,J.J., Croteau,D.L., Van Houten,B. and Kisker,C. (2006) Prokaryotic nucleotide excision repair: the UvrABC system. *Chem. Rev.*, **106**, 233–252.
3. Theis,K., Chen,P.J., Skorvaga,M., Van Houten,B. and Kisker,C. (1999) Crystal structure of UvrB, a DNA helicase adapted for nucleotide excision repair. *EMBO J.*, **18**, 6899–6907.
4. Skorvaga,M., Theis,K., Mandavilli,B.S., Kisker,C. and Van Houten,B. (2002) The beta -hairpin motif of UvrB is essential for DNA binding, damage processing, and UvrC-mediated incisions. *J. Biol. Chem.*, **277**, 1553–1559.
5. Truglio,J.J., Karakas,E., Hau,B., Wang,H., DellaVecchia,M.J., Van Houten,B. and Kisker,C. (2006) Structural basis for DNA recognition and processing by UvrB. *Nat. Struct. Mol. Biol.*, **13**, 360–364.
6. Waters,T.R., Eryilmaz,J., Geddes,S. and Barrett,T.E. (2006) Damage detection by the UvrABC pathway: crystal structure of UvrB bound to fluorescein-adducted DNA. *FEBS Lett.*, **580**, 6423–6427.
7. Malta,E., Moolenaar,G.F. and Goosen,N. (2006) Base flipping in nucleotide excision repair. *J. Biol. Chem.*, **281**, 2184–2194.
8. Malta,E., Verhagen,C.P., Moolenaar,G.F., Filippov,D.V., Van der Marel,G.A. and Goosen,N. (2008) Functions of base flipping in *E. coli* nucleotide excision repair. *DNA Repair*, **7**, 1647–1658.
9. Pakotiprapha,D., Inuzuka,Y., Bowman,B.R., Moolenaar,G.F., Goosen,N., Jeruzalmi,D. and Verdine,G.L. (2008) Crystal structure of *Bacillus stearothermophilus* UvrA provides insight into ATP-modulated dimerization, UvrB interaction, and DNA binding. *Mol. Cell*, **29**, 122–133.
10. Hopfner,K.P. and Tainer,J.A. (2003) Rad50/SMC proteins and ABC transporters: unifying concepts from high resolution structures. *Curr. Opin. Struct. Biol.*, **13**, 249–255.

11. Oh,E.Y., Claassen,L., Thiagalingam,S., Mazur,S. and Grossman,L. (1989) ATPase activity of the UvrA and UvrAB protein complexes of the *Escherichia coli* UvrABC endonuclease. *Nucleic Acids Res.*, **17**, 4145–4159.
12. Orren,D.K. and Sancar,A (1989) The (A)BC excinuclease of *Escherichia coli* has only the UvrB and UvrC subunits in the incision complex. *Proc. Natl Acad. Sci. USA*, **86**, 5237–5241.
13. Van Houten,B., Gamper,H., Sancar,A. and Hearst,J.E. (1987) DNaseI footprint of ABC excinuclease. *J. Biol. Chem.*, **262**, 13180–13187.
14. Seeberg,E. and Steinum,A. L. (1982) Purification and properties of the UvrA protein from *Escherichia coli*. *Proc. Natl Acad. Sci. USA.*, **79**, 988–992.
15. Van Houten,B., Gamper,H., Hearst,J.E. and Sancar,A. (1988) Analysis of sequential steps of nucleotide excision repair in *Escherichia coli* using synthetic substrates containing single psoralen adducts. *J. Biol. Chem.*, **263**, 16553–16560.
16. Mazur,S. and Grossman,L. (1991) Dimerization of *Escherichia coli* UvrA and its binding to undamaged and ultraviolet damaged DNA. *Biochemistry*, **30**, 4432–4443.
17. Thiagalingam,S. and Grossman,L. (1993) The multiple roles for ATP in the *Escherichia coli* UvrABC endonuclease-catalyzed incision reaction. *J. Biol. Chem.*, **268**, 18382–18389.
18. Visse,R., de Ruijter,M., Moolenaar,G.F. and van de Putte,P. (1992) Analysis of UvrABC endonuclease reaction intermediates on cis-platin-damaged DNA using mobility shift gel electrophoresis. *J. Biol. Chem.*, **267**, 6736–6742.
19. Verhoeven,E.E.A., Wyman,C., Moolenaar,G.F., Hoeijmakers,J.H.J. and Goosen,N. (2001) Architecture of nucleotide excision repair complexes: DNA is wrapped by UvrB before and after damage recognition. *EMBO J.*, **20**, 601–611.
20. Horcas,I., Fernandez,R., Gomez-Rodriguez,J.M., Colchero,J., Gomez-Herrero,J. and Baro,A.M. (2007) WSXM: a software for scanning probe microscopy and a tool for nanotechnology. *Rev. Sci. Instrum.*, **78**, 013705.
21. Ratcliff,G.C. and Erie,D.A. (2001) A novel single-molecule study to determine protein-protein association constants. *J. Am. Chem. Soc.*, **123**, 5632–5635.
22. Yang,Y., Sass,L.E., Du,C., Hsieh,P. and Erie,D.A. (2005) Determination of protein-DNA binding constants and specificities from statistical analyses of single molecules: MutS-DNA interactions. *Nucleic Acids Res.*, **33**, 4322–4334.
23. Myles,G.M., Hearst,J.E. and Sancar,A. (1991) Site-specific mutagenesis of conserved residues within Walker A and B sequences of *Escherichia coli* UvrA protein. *Biochemistry*, **30**, 3824–3834.
24. Wang,H., DellaVecchia,M.J., Skorvaga,M., Croteau,D.L., Erie,D.A. and Van Houten,B. (2006) UvrB domain 4, an autoinhibitory gate for regulation of DNA binding and ATPase activity. *J. Biol. Chem.*, **281**, 15227–15237.
25. Verhoeven,E.E.A., Wyman,C., Moolenaar,G.F. and Goosen,N. (2002) The presence of two UvrB subunits in the UvrAB complex ensures damage recognition in both DNA strands. *EMBO J.*, **21**, 4196–4205.
26. Wang,H., Tessmer,I., Croteau,D.L., Erie,D.A. and Van Houten,B. (2008) Functional characterization and atomic force microscopy of a DNA repair protein conjugated to a quantum dot. *Nano Lett.*, **8**, 1631–1637.
27. Malta,E., Moolenaar,G.F. and Goosen,N. (2007) Dynamics of the UvrABC nucleotide excision repair proteins analyzed by fluorescence resonance energy transfer. *Biochemistry*, **46**, 9080–9088.